

Supporting Information

**Bacitracin-engineered BSA/ICG nanocomplex with enhanced
photothermal and photodynamic antibacterial activity**

Yueying Xu,^{a1} Wenhong Zhou,^{a1} Le Xiao,^{a1} Qian Lan,^a Mingen Li,^a Yun Liu,^a Lijun Song,^{a,*} and Li Li^{a,*}

^a Guangdong Key Laboratory for Research and Development of Natural Drugs, School of Pharmacy, Guangdong Medical University, 524023, Zhanjiang, China

*Correspondence: Email: songlijun6981@126.com (LS); china_lovelylily@hotmail.com (LL);

¹These authors contributed equally to this work.

Corresponding author.

E-mail address: songlijun6981@126.com

Corresponding author.

E-mail address: china_lovelylily@hotmail.com

Figure S1: Particle size distribution of BSA@ICG, and stability of BSA@ICG@Bac in water and PBS 7.4

Figure S2: Drug loading of ICG in BSA@ICG@Bac

Figure S3: Effect of water on the UV-absorption spectrum of DPBF under 808 nm laser irradiation and the effect of BSA@ICG@Bac in dark

Figure S4: Absorption intensity under different conditions

Figure S5: Photothermal conversion efficiency of BSA@ICG@Bac

Figure S6: FTIR spectra of the raw materials forming BSA@ICG@Bac and BSA@ICG@Bac

Figure S7: Photothermal imaging of BSA@ICG@Bac at different concentrations

Figure S8: In vitro antimicrobial activity of BSA@ICG and BSA@ICG@Bac with or without 660 nm laser irradiation

Figure S9: Targeting of BSA@ICG and BSA@ICG@Bac by *S. aureus*

Figure S10: Fluorogram of intracellular production of reactive oxygen species by *S. aureus*

Figure S11: Photographs of *S. aureus* and *E. coli* biofilms

Table S1: MIC of BSA@ICG@Bac

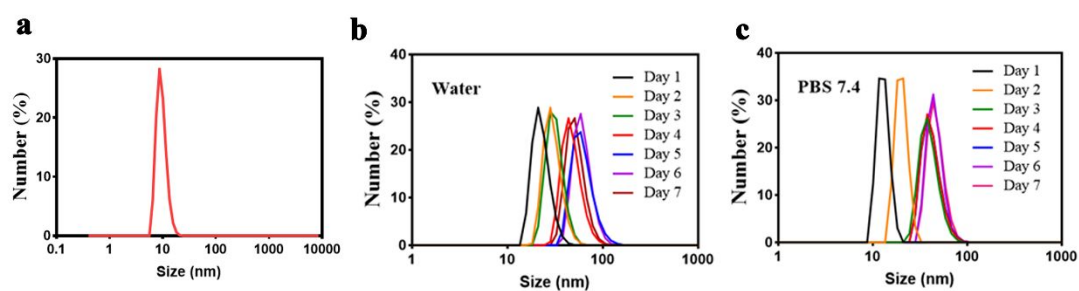


Figure S1. (a) BSA@ICG NPs measured by dynamic light scattering (DLS). Hydrodynamic diameters of BSA@ICG@Bac in (b) water and (c) PBS 7.4 during 7 days obtained by dynamic light scattering.

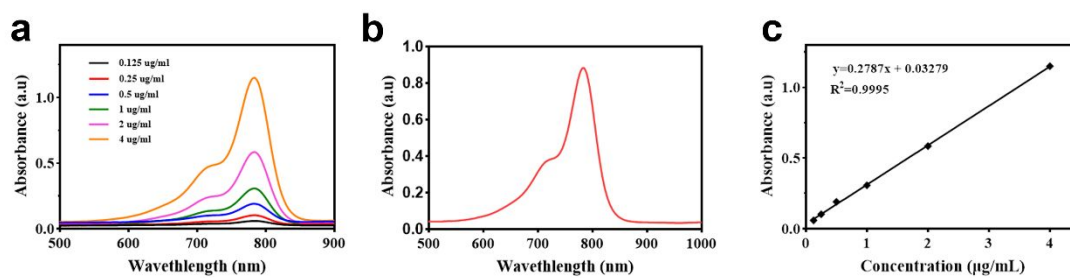


Figure S2. (a) UV-Vis spectra of ICG dispersion with different concentrations. (b) UV-Vis spectra of free ICG diluted 16 times. (c) liner fitting curve. According to equation the loading content is calculated to be 6.6 %, and the encapsulation efficiency is 80.5%.

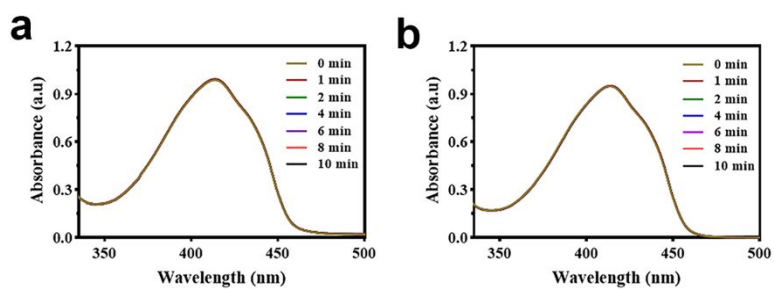


Figure S3. Spectrogram of UV absorption of DPBF with (a) H₂O under 808 nm irradiation and (b) BSA@ICG@Bac without 808 nm irradiation.

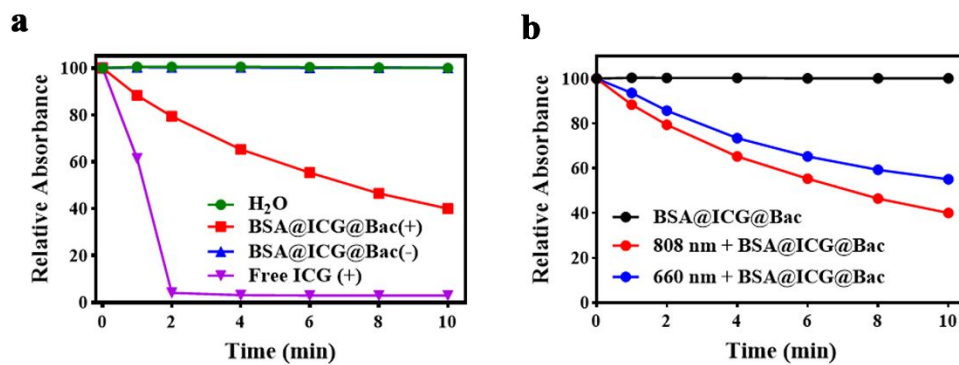


Figure S4. (a) Absorption strength of the different sample groups under 808 nm irradiation. (b) Absorption strength under different laser irradiation.

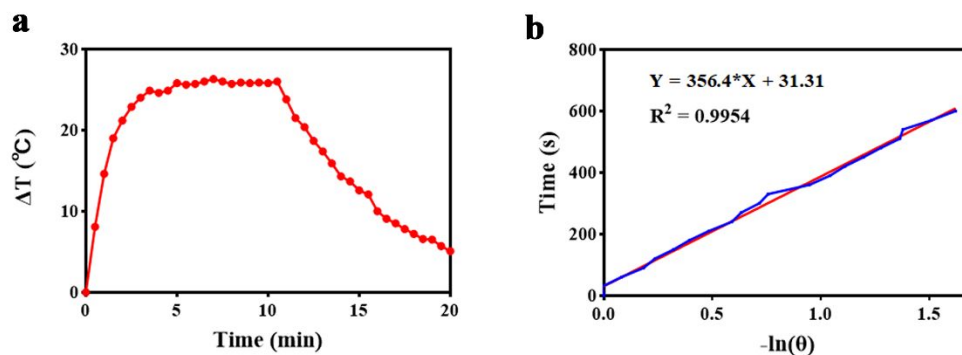


Figure S5. (a) Photothermal effect of aqueous dispersion of nanoparticles under irradiation with the NIR laser for one on/off cycle. (b) Time constant for heat transfer from the system. The value of photothermal conversion efficiency (η) was calculated according the equation, $\eta = \frac{hs(T_{max} - T_{max, water})}{I(1 - 10^{-A_{\lambda}})}$. In this equation, hs was $0.0118 \text{ J}/(\text{kg}\cdot\text{K}\cdot\text{s})$, which was measured by fitting the cooling curve of BSA@ICG@Bac NPs solution. The maximum steady temperature (T_{max}) was $57 \text{ }^{\circ}\text{C}$ and the ambient environmental temperature ($T_{max, water}$) was $35.5 \text{ }^{\circ}\text{C}$. The power density of laser (I) was $1 \text{ W}/\text{cm}^2$. The absorbance of BSA@ICG@Bac NPs solution (A_{λ}) was 0.631 , which was measured using quartz cell containing aqueous samples without BSA@ICG@Bac NPs. Thus, according to equation, the photothermal conversion efficiency (η) of the BSA@ICG@Bac NPs at 808 nm is calculated to be 33.07% .

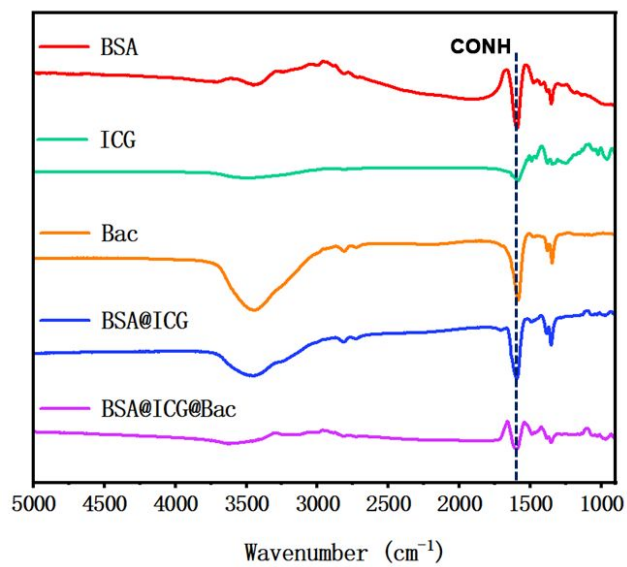


Figure S6. FT-IR spectra of BSA, ICG, Bacitracin (Bac), BSA@ICG and BSA@ICG@Bac NPs.

The vibration peaks at 1600 cm⁻¹ match with the CONH groups of BSA.

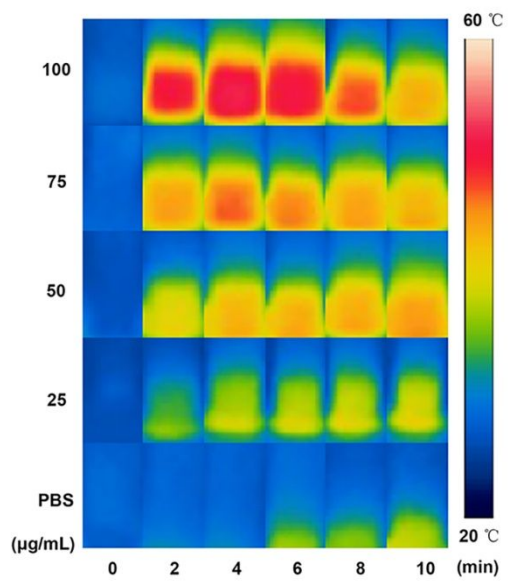


Figure S7. Photothermal heating diagram of BSA@ICG@Bac at different concentrations at 1 W /cm² under 808 nm irradiation.

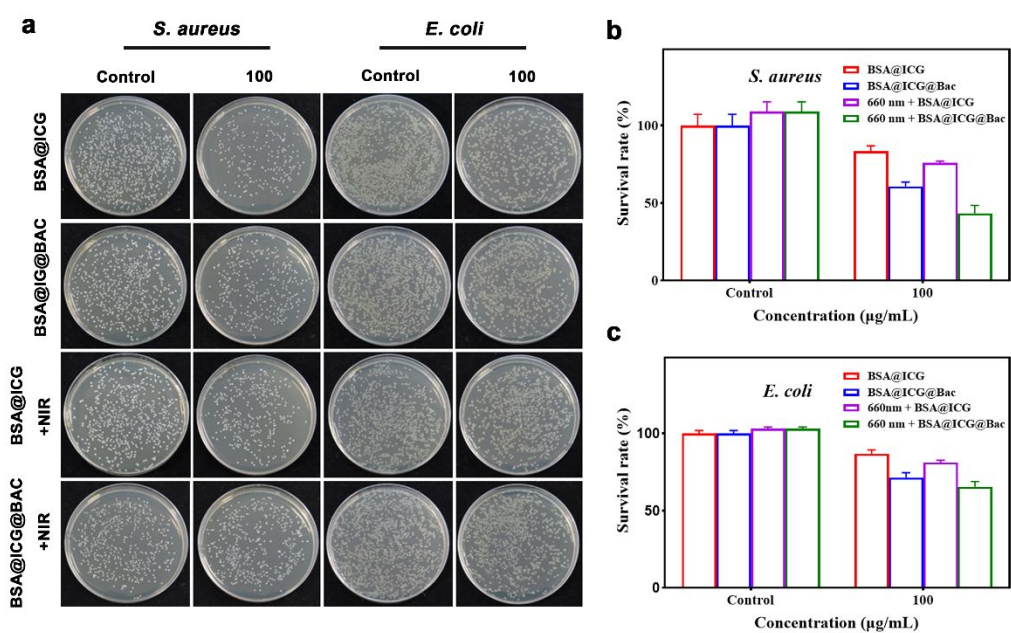


Figure S8. Photographs of bacterial colonies formed by (a) *S. aureus* and *E. coli* treated with different concentration of BSA@ICG and BSA@ICG@Bac with or without 660 nm irradiation at 1 W /cm². The bacterial survival of (b) *S. aureus* and (c) *E. coli* after treatment determined by the plate counting method.

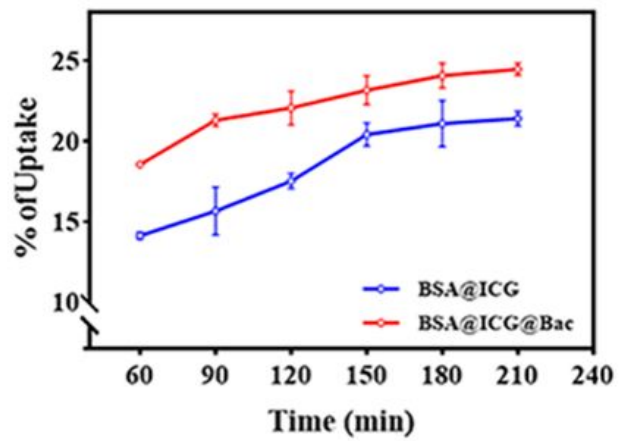


Figure S9. Uptake percentages of BSA@ICG and BSA@ICG@Bac by *S. aureus*.

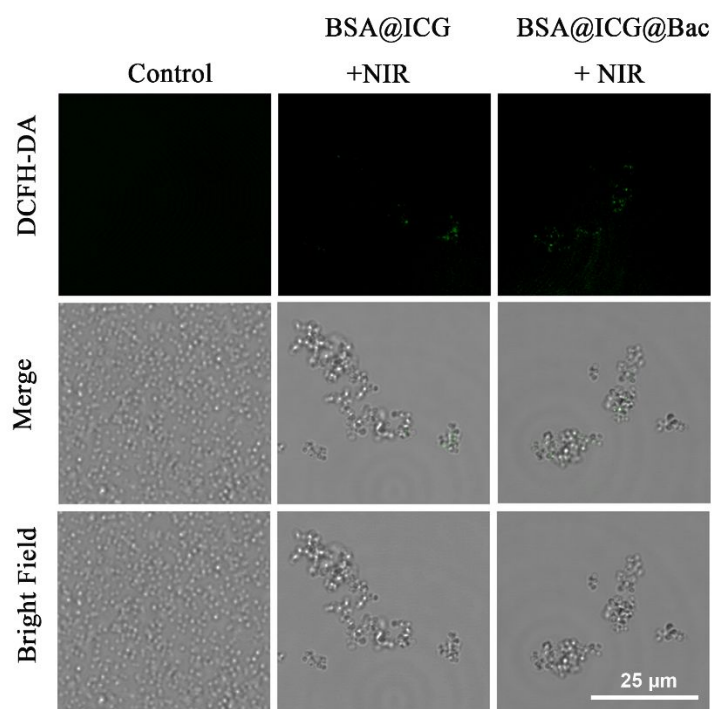


Figure S10. ROS production in *S. aureus* after being exposed to BSA@ICG and BSA@ICG@Bac NPs under 808 nm irradiation.

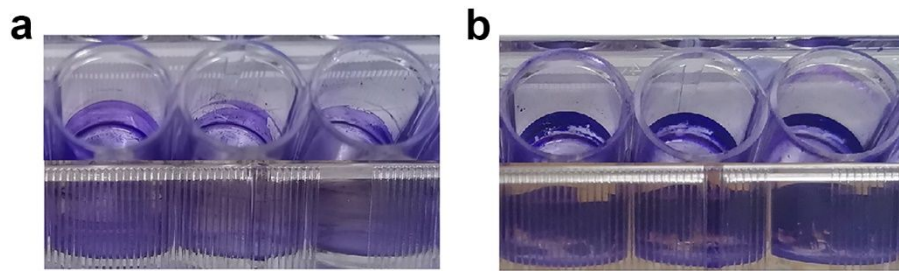


Figure S11. (a) *S. aureus* and (b) *E. coli* biofilms were stained by crystal violet.

Table S1Antimicrobial activity of BSA@ICG@Bac NPs as MIC ($\mu\text{g/mL}$).

	Bacteria	
	<i>S. aureus</i>	<i>E. coli</i>
BSA@ICG@Bac (-)	R	R
BSA@ICG@Bac (+)	100	100

R, resistant